

DOI: 10.1002/adma.200602906

# A Germanium Inverse Woodpile Structure with a Large Photonic Band Gap\*\*

By Florencio García-Santamaría, Mingjie Xu, Virginie Lousse, Shanhui Fan, Paul V. Braun,\* and Jennifer A. Lewis\*

The fabrication of 3D structures with a large complete photonic bandgap (PBG) has been an important goal, since the concept was introduced two decades ago.<sup>[1,2]</sup> Many proposed structures exhibit PBGs with theoretical relative widths<sup>[3]</sup> below 5 %, often too narrow for practical applications,<sup>[4]</sup> since structural inhomogeneities may reduce the size, or even close, PBGs<sup>[5]</sup> by introducing unwanted modes into the band structure. In this letter, we report the simulation, assembly, and optical properties of the first Ge inverse woodpile structure with a 25 % wide PBG. This structure is created by direct-write assembly of a polymeric template followed by sequential deposition of a sacrificial oxide bilayer and Ge. The photonic response is maximized by tuning the Ge filling fraction in accordance with theoretical predictions. Upon removal of the template and sacrificial layers, the reflectance spectrum acquired from the resulting Ge inverse woodpile structure shows a large reflectance peak in the mid-IR indicative of a PBG.

3D periodic structures with a diamond symmetry offer a promising approach for creating PBG materials.<sup>[6]</sup> Among the

diamond<sup>[7]</sup> or diamondlike<sup>[8–11]</sup> lattices that have been fabricated to date, the woodpile structure introduced by Ho et al.<sup>[12]</sup> remains the most popular.<sup>[13]</sup> This structure is composed of dielectric rods stacked in a periodic array such that their contact points form a diamondlike lattice. A great advantage of the woodpile architecture over other structures is that it can be readily fabricated by standard lithographic techniques.<sup>[14,15]</sup> However, the production of high quality, three-dimensional lattices is expensive. Hence, the study of these crystals has been rather limited. Alternate strategies, such as direct laser<sup>[16]</sup> and ink writing,<sup>[17]</sup> have been introduced to create inexpensive polymeric woodpile templates, and very recently, in two simultaneous publications, we<sup>[18]</sup> and Ozin et al.<sup>[19]</sup> demonstrated their conversion to high-refractive-index, photonic crystals.

Until our recent efforts,<sup>[18]</sup> all woodpile structures have been composed of solid dielectric rods in an air matrix,<sup>[14,15,19,20]</sup> even though it is known that inverse symmetries consisting of air rods in a high-refractive-index matrix offer significant advantages. Not only are their PBGs wider, but lower dielectric filling fractions are required to maximize the gap width.<sup>[12]</sup> Such low filling fractions are advantageous, since the PBG occurs at higher frequencies for a given lattice parameter.

In this Communication, we report the first realization and characterization of a Ge inverse woodpile structure with a theoretical PBG width as large as 25 %. As proposed in the literature,<sup>[12]</sup> the woodpile structure with the largest PBG consists of interpenetrating air rods in a high-refractive-index material. In the case of Ge ( $n = 4.1$ ), a 31 % wide PBG can be obtained at the optimal filling fraction. However, this structure cannot be realized experimentally via templating routes, since conformal growth of high-refractive-index material leads to the formation of isolated pores that limit the Ge filling fraction. For cylindrical rods, this threshold value occurs when the outer radius equals  $0.306a$ , where  $a$  is the lattice parameter. Yet, even in the presence of these isolated pores, the inverse woodpile structure can display a large (25 % wide) PBG. Figure 1a shows the band structure and density of states<sup>[21]</sup> of an inverse Ge photonic crystal made of interpenetrated hollow cylinders with internal and external radii of  $r_i = 0.25a$  and  $r_e = 0.306a$ , respectively. These values, corresponding to a Ge filling fraction of 0.16, yield a gap centered at  $a/\lambda = 0.565$ , where  $\lambda$  is the wavelength. Figure 1b shows how the internal radius of the rods and, therefore, the filling fraction, can be

[\*] Prof. P. V. Braun, Prof. J. A. Lewis, Dr. F. García-Santamaría  
Department of Materials Science and Engineering  
Frederick Seitz Materials Research Laboratory, Beckman Institute  
University of Illinois at Urbana-Champaign  
Urbana, IL 61801 (USA)  
E-mail: pbraun@uiuc.edu; jalewis@uiuc.edu

Prof. J. A. Lewis, M. Xu  
Department of Chemical and Biomolecular Engineering  
Urbana, IL 61801 (USA)

Dr. V. Lousse, Prof. S. Fan  
Department of Electrical Engineering, Stanford University  
Stanford, CA 94305-4088 (USA)

Dr. V. Lousse  
Laboratoire de Physique du Solide  
Facultés Universitaires Notre-Dame de la Paix  
5000 Namur (Belgium)

[\*\*] F.G.-S. and M.X. contributed equally to this work. This material is based in part on work supported by the U.S. Department of Energy, Division of Materials Sciences, under Award No. DEFG-02-91ER45439, through the Frederick Seitz Materials Research Laboratory at the University of Illinois at Urbana-Champaign (UIUC), and the U.S. Army Research Laboratory and the U.S. Army Research Office under contract/grant number DAAD19-03-1-0227, and was carried out in part in the Center for Microanalysis of Materials, UIUC, which is partially supported by the U.S. Department of Energy under grant DEFG02-91-ER45439.

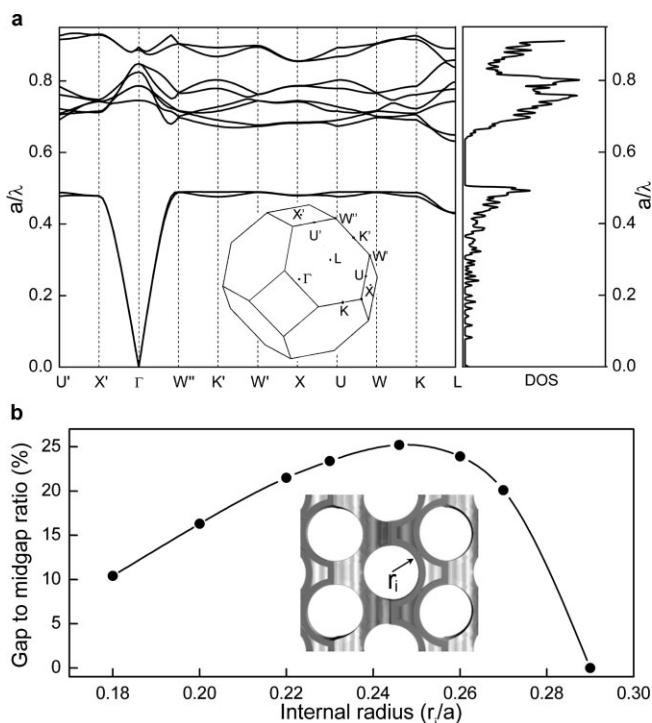


**Figure 1.** a) Band structure and density of states of an inverse woodpile structure consisting of hollow Ge ( $n=4.1$ ) tubes with an internal radius of  $0.25a$  and an external radius of  $0.306a$ . The inset shows the Brillouin zone and its most important symmetry points. b) Dependence of the gap to midgap ratio as a function of the internal radius of these hollow tubes. The inset shows a (100) facet where the internal radius of the hollow rods is depicted.

adjusted to optimize the gap width. Note, even significant deviations from this optimal value still yield a large PBG.

To create a Ge inverse woodpile structure with the theoretical photonic properties shown in Figure 1a, we first produce a polymer scaffold by using direct-write assembly<sup>[17]</sup> of a concentrated polyelectrolyte ink.<sup>[22]</sup> A homogeneous fluidic ink (40 wt % polyelectrolyte in aqueous solution) is deposited into an alcohol-rich reservoir to produce a cylindrical filament approximately 1  $\mu\text{m}$  in diameter that is patterned in a layer-by-layer build sequence. This polymer woodpile structure consists of 12 layers with overall lateral dimensions of  $200\text{ }\mu\text{m} \times 200\text{ }\mu\text{m}$ . The in-plane lattice parameter,  $a$ , is 4  $\mu\text{m}$  with a center-to-center rod spacing  $d$  of  $a/\sqrt{2} \approx 2.8\text{ }\mu\text{m}$  (Fig. 2a). To maximize the width of the PBG, a 500 nm sacrificial oxide bilayer (Fig. 2b) is conformally deposited around the polymer cylinders via a combination of atomic layer deposition (ALD) and chemical vapor deposition (CVD). Next, a 225 nm thick layer of amorphous Ge is deposited by using CVD (Fig. 2c). Since the gaseous precursor,  $\text{Ge}_2\text{H}_6$ , used during CVD decomposes to form amorphous Ge at ca. 250 °C, the polymer rods do not have to be removed prior to this step. This low growth temperature, along with the high dielectric constant of Ge, offer significant advantages over Si.<sup>[18]</sup> Finally, the polymer template is removed by thermal decomposition at 475 °C followed by removal of the sacrificial oxide layers

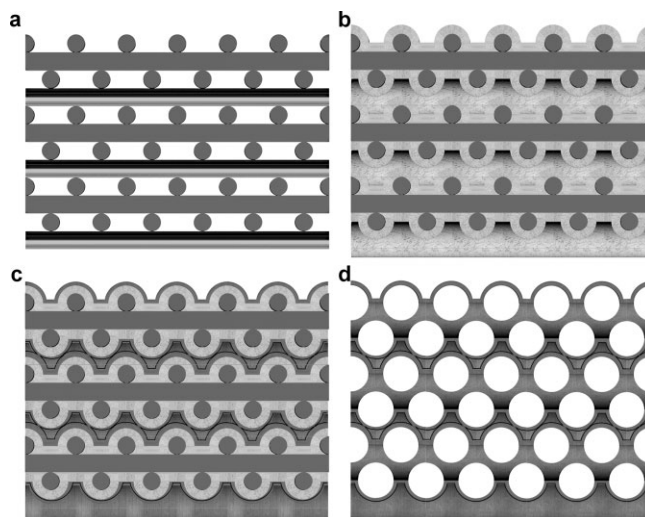


**Figure 2.** Fabrication scheme. a) Initial polymeric woodpile structure created by direct ink writing; b) thick film of an oxide bilayer conformally grown around the polymeric rods via ALD and CVD; c) infilling of the remaining pore volume with Ge via CVD; d) removal of the oxide and polymeric materials to yield a Ge inverse woodpile structure.

using a HF etchant to yield the Ge inverse woodpile photonic crystal shown in Figure 2d.

Scanning electron microscopy (SEM) images of the resulting Ge inverse woodpile structure are shown in Figure 3. This cross-sectional view is obtained by focused ion beam (FIB) milling. Figure 3b and c depicts the (100) and (110) planes, respectively, while Figure 3d and e are the corresponding computer renderings of the (100) and (110) planes for direct comparison. Overall, there is excellent agreement between the two sets of images. The mixture of orientations observed in Figure 3b reflects the fact that the FIB cross sections are not perfectly parallel to these planes. In fact, rather different geometries are observed depending on the exact position where these sections are obtained, as shown in Figure 3f and g.

To characterize the optical response of the Ge inverse woodpile photonic crystals, and relate it to the properties of the initial polymer template, optical characterization is performed at each step of the fabrication process (Fig. 4). Figure 4a shows the reflectance spectrum from the polymer template ( $a = 3.8\text{ }\mu\text{m}$ ). The peak near 4  $\mu\text{m}$  corresponds to the first stop band and has a maximum reflectance of 0.35. This value represents a two-fold improvement over prior polymer woodpile structures created by using direct ink writing,<sup>[18]</sup> demonstrating that high-quality templates can be produced by using this approach. The presence of well-defined optical features around 2  $\mu\text{m}$  is also remarkable, since optical features at shorter wavelengths are suppressed by structural inhomogeneities. Figure 4b presents the reflectance spectra for the oxide-coated, polymer woodpile structure. The peaks red-shift slightly, although not as much as might be expected given the oxide bilayer thickness. This is due to the slight contraction of the lattice during  $\text{Al}_2\text{O}_3$  ALD, which occurs at 180 °C. Calculations indicate the lattice parameter is reduced by 7 % during this

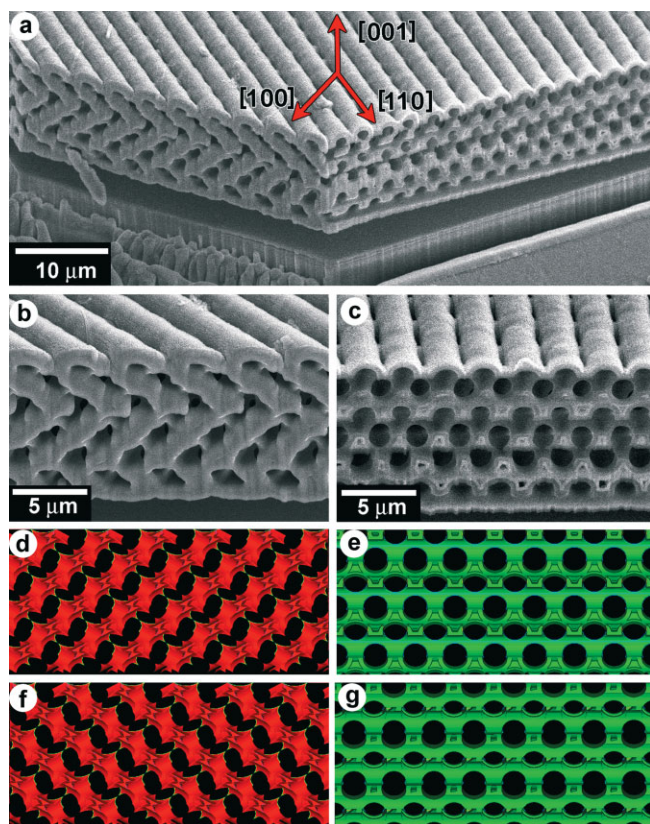


**Figure 3.** Inverse Ge woodpile structure. a) SEM image showing the surface of the sample with two edges exposed by FIB milling, with their orientations indicated. b, c) SEM higher resolution images of exposed (100) and (110) planes, respectively. Both images are taken with the substrate tilted 55°. d, e) Computer-rendered images of the edges shown in (b) and (c), equivalently tilted at 55°. f, g) Cross-sectional cuts at slightly different positions also parallel to the (100) and (110) planes, respectively.

process (3.80 to 3.53  $\mu\text{m}$ ). Once Ge is deposited by using CVD, the reflectance dramatically increases, and the spectra becomes more complex (Fig. 4c). The stop band significantly redshifts despite the fact that the sample is only 16 % Ge by volume. Upon removal of the polymer template and the sacrificial oxide bilayer (Fig. 4d), the optical features blue-shift as expected, and more importantly, the peak centered at 6  $\mu\text{m}$  significantly broadens. It is this optical feature that corresponds to the theoretically predicted, large PBG associated with the Ge inverse woodpile structure; the theoretical spectral position and width of the complete PBG is denoted by the shaded region in Figure 4d. The experimental spectrum (thick line) is compared to the results simulated using the transfer-matrix method<sup>[23]</sup> (thin line), and other than the absolute magnitude of the reflectance, the correspondence is quite good. In the experiment, reflectance is not unity due to diffuse scattering from the surface roughness, which is best observed in Figure 3c, coming from the deposition of unwanted particles during the Ge CVD process. Combining simulation and experiment, we have demonstrated a new route for creating three-dimensional complete bandgap photonic crystals at IR wavelengths.

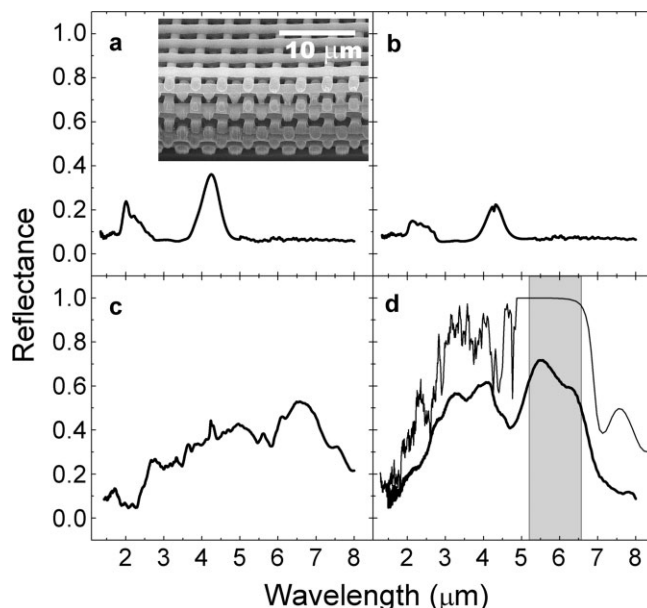


**Figure 4.** Reflectance spectra at different stages of fabrication. a) Initial polymer woodpile structure (inset shows an SEM cross section); b) oxide-coated polymer woodpile structure; c) Ge/oxide-coated, polymer woodpile structure; d) experimental (thick line) and simulated (thin line) Ge inverse woodpile structure. The lightly shaded region depicts the PBG.

In summary, we have created Ge inverse woodpile structures that can exhibit a complete PBG as large as 25 % when properly designed. Due to the low Ge filling fraction and inverse configuration, this architecture allows one to open up larger PBGs at shorter wavelengths than for the direct woodpile structure. Our approach can be readily adopted for converting other polymeric woodpile templates, such as those fabricated by using laser-writing,<sup>[16]</sup> electron-beam lithography,<sup>[20]</sup> or phase-contrast lithography,<sup>[24]</sup> into inverse woodpile structures. In addition to their potential as photonic materials, these interconnected, inverse woodpile structures may find potential application as low-cost microelectromechanical systems,<sup>[25]</sup> microfluidic networks for heat dissipation,<sup>[26]</sup> and biological devices.<sup>[27]</sup>

## Experimental

**Fabrication:** Polymeric scaffolds were produced by direct-write assembly of a concentrated polyelectrolyte ink on a  $\text{HfO}_2$ -coated glass slide following a procedure reported in the literature [18,22]. After fabrication, the scaffolds were dried at 22 °C in a low-humidity environment (15–28 % relative humidity). Samples were then heated to 180 °C and held for 3 h. A commercial ALD system (Cambridge Nanotech) was used to conformally grow 20 nm of  $\text{Al}_2\text{O}_3$  at 180 °C onto the polymer scaffold using water vapor and trimethylaluminum as precursors with dosing times of 0.05 and 0.1 s, respectively, for 200 cycles. Next, a 480 nm thick coating of  $\text{SiO}_2$  was deposited using CVD under ambient temperature and pressure [28]. Water-saturated  $\text{N}_2$  was first allowed to flow over the structure for 90 s to hydrate the sample; this was followed by  $\text{SiCl}_4(\text{g})$ -saturated  $\text{N}_2$  at a rate of 6  $\text{mL min}^{-1}$  for 90 s. An  $\text{Al}_2\text{O}_3/\text{SiO}_2$  bilayer coating was used because the  $\text{Al}_2\text{O}_3$  layer

offers higher mechanical and thermal stability than the SiO<sub>2</sub> layer obtained by using CVD, preventing sample cracking during subsequent processing steps. However, ALD was not suitable for growing thick coatings (> 100 nm), so, a combination of the two deposition methods was utilized. The oxide-coated, polymer scaffolds were then placed in a furnace at 200 °C overnight to densify the silica film. The total oxide thickness was monitored by using SEM (Hitachi S-4700). Ge was then grown on the scaffold surface via CVD using Ge<sub>2</sub>H<sub>6</sub> as the precursor gas [29]. The sample was loaded into a reaction vessel and isolated at ca. 20 mbar (1 bar = 100 000 Pa). The reaction vessel was then inserted into a vertical-tube furnace set at 250 °C. The decomposition reaction proceeded for 15 h, depositing amorphous Ge on the surface of the cylinders. This cycle was repeated three times to obtain a total film thickness of ca. 200 nm. Before thermally decomposing the polymer, the Ge/oxide/polymer structure was covered with an ca. 100 nm layer of SiO<sub>2</sub> to prevent Ge oxidation. A vertical cross section of a Ge-oxide composite scaffold was exposed by using FIB (FEI dual-beam DB-235) milling. The ion currents employed for etching and cleaning in FIB were 3000 and 500 pA, respectively. The polymer core was removed by heat treatment at 475 °C in air for 1 h. The oxide layers were then removed by using a 10 % solution of HF(aq) in ethanol (two cycles of 15 min each) and rinsed with ethanol.

**Optics:** Reflectance spectra were measured using a global lamp and 15X Cassegrain objectives with a numerical aperture of 0.4. Light impinged the sample at an angle centered around 16.7° with respect to the sample normal. The collection area was limited to a 50 µm diameter circle using an aperture in the image plane of the optical path. The signal is coupled to a Fourier transform IR (FTIR, Vertex 70, Bruker) system with a mercury–cadmium–telluride detector. Spectra were normalized to a gold mirror.

**Simulations:** The spectrum simulation was done using the transfer-matrix method in a momentum-space representation. Our calculation contains the full polarization information and accounts for the acceptance angles of the Cassegrain objective described above. Simulations matched the actual spectroscopic conditions and included all azimuthal angles and polarizations. The inverse woodpile structure was simulated assuming hollow Ge ( $n = 4.1$ ) rods with an internal and external diameter of 1.8 and 2.2 µm, respectively. The layer-to-layer spacing in the  $z$ -direction was set to 900 nm. The effect of the glass substrate ( $n = 1.5$ ) was taken into consideration.

Received: December 20, 2006  
Published online: May 18, 2007

- [1] E. Yablonovitch, *Phys. Rev. Lett.* **1987**, *58*, 2059.
- [2] S. John, *Phys. Rev. Lett.* **1987**, *58*, 2486.
- [3] The gap size is defined as the full width at half maximum divided by the center value of the gap.
- [4] A. Blanco, E. Chomski, S. Grabtchak, M. Ibisate, S. John, S. W. Leonard, C. López, F. Meseguer, H. Míguez, J. P. Mondia, G. A. Ozin, O. Toader, H. M. van Driel, *Nature* **2000**, *405*, 437.
- [5] M. M. Sigalas, C. M. Soukoulis, C. T. Chan, R. Biswas, K. M. Ho, *Phys. Rev. B* **1999**, *59*, 12 767.
- [6] M. Maldovan, E. L. Thomas, *Nat. Mater.* **2004**, *3*, 593.
- [7] F. García-Santamaría, H. T. Miyazaki, A. Urquía, M. Ibisate, M. Belmonte, N. Shinya, F. Meseguer, C. López, *Adv. Mater.* **2002**, *14*, 1144.
- [8] E. Yablonovitch, T. J. Gmitter, K. M. Leung, *Phys. Rev. Lett.* **1991**, *67*, 2295.
- [9] O. Toader, S. John, *Phys. Rev. E* **2002**, *66*, 016610.
- [10] E. Schubert, T. Hoche, F. Frost, B. Rauschenbach, *Appl. Phys. A* **2005**, *81*, 481.
- [11] J. H. Moon, S. Yang, D. J. Pine, S. M. Yang, *Opt. Express* **2005**, *13*, 9841.
- [12] K. M. Ho, C. T. Chan, C. M. Soukoulis, R. Biswas, M. Sigalas, *Solid State Commun.* **1994**, *89*, 413.
- [13] This lattice was originally termed ‘layer-by-layer’, however, more frequently it is described as ‘woodpile’. We have chosen the latter terminology in this Communication.
- [14] J. G. Fleming, S. Y. Lin, *Opt. Lett.* **1999**, *24*, 49.
- [15] N. Yamamoto, S. Noda, A. Chutinan, *Jpn. J. Appl. Phys. Part 2* **1998**, *37*, 1491.
- [16] M. Deubel, G. von Freymann, M. Wegener, S. Pereira, K. Busch, C. M. Soukoulis, *Nat. Mater.* **2004**, *3*, 444.
- [17] G. M. Gratson, M. J. Xu, J. A. Lewis, *Nature* **2004**, *428*, 386.
- [18] G. M. Gratson, F. García-Santamaría, V. Lousse, M. Xu, S. H. Fan, J. A. Lewis, P. V. Braun, *Adv. Mater.* **2006**, *18*, 461.
- [19] N. Tétreault, G. von Freymann, M. Deubel, M. Hermatschweiler, F. Pérez-Willard, S. John, M. Wegener, G. A. Ozin, *Adv. Mater.* **2006**, *18*, 457.
- [20] G. Subramania, S. Y. Lin, *Appl. Phys. Lett.* **2004**, *85*, 5037.
- [21] The eigenstates are computed using a plane wave basis in an iterative implementation (MIT Photonics-Bands (MPB) package v-1.4.2) as described in: S. G. Johnson, J. D. Joannopoulos, *Opt. Express* **2001**, *8*, 173.
- [22] G. M. Gratson, J. A. Lewis, *Langmuir* **2005**, *21*, 457.
- [23] J. B. Pendry, A. Mackinnon, *Phys. Rev. Lett.* **1992**, *69*, 2772.
- [24] S. Jeon, V. Malyarchuk, J. A. Rogers, G. P. Wiederrecht, *Opt. Express* **2006**, *14*, 2300.
- [25] T. Yamamoto, J. Yamaguchi, N. Takeuchi, A. Shimizu, R. Sawada, E. Higurashi, Y. Uenishi, *Jpn. J. Appl. Phys. Part 1* **2004**, *43*, 5824.
- [26] J. M. Koo, S. Im, L. N. Jiang, K. E. Goodson, *J. Heat Transfer* **2005**, *127*, 49.
- [27] A. Ressine, S. Ekstrom, G. Marko-Varga, T. Laurell, *Anal. Chem.* **2003**, *75*, 6968.
- [28] H. Míguez, N. Tétreault, B. Hatton, S. M. Yang, D. Perovic, G. A. Ozin, *Chem. Commun.* **2002**, 2736.
- [29] H. Míguez, E. Chomski, F. García-Santamaría, M. Ibisate, S. John, C. López, F. Meseguer, J. P. Mondia, G. A. Ozin, O. Toader, H. M. van Driel, *Adv. Mater.* **2001**, *13*, 1634.